# THREE-DIMENSIONAL NUMERICAL ANALYSIS OF SEDIMENT TRANSPORT AROUND ABUTMENTS IN CHANNEL BEND

Han Sang Kim[1] and Hamn-Ching Chen[1]

In this paper, the results for sediment transport simulation around bridge abutments in a channel bend are presented. Computational Fluid Dynamics code FANS3D is used to conduct the study, which solves three-dimensional Reynolds-Averaged Navier-Stokes equations with the finite analytic scheme. The two-layer turbulence model, which combines the one- and two-equation eddy-viscosity models, is utilized to resolve turbulence near smooth solid surfaces. The wall-function approach is adopted to take into account the roughness effects in case of sediment beds. For velocity-pressure coupling, PISO/SIMPLER algorithms are used. Chimera technique is utilized to embed non-matching blocks in the computational domain. The numerical model coupled with the sediment transport module was validated with experimental studies. For the present case, the transport of suspended sediment in a 90°-channel bend with abutments located in the middle was simulated. Sediment plume in a swirl was observed downstream of the abutments.

Keywords: sediment transport; computational fluid dynamics; abutment scouring

## INTRODUCTION

Predicting sediment transport has numerous implications in coastal engineering and related fields, including port and harbor management and design of hydraulic structures. Buildup of sediments in navigational channels pose great threat to vessels (Sanchez-Badorrey et al., 2008). Excessive sediment layers require dredging, which may become a considerable economic burden (Miller, 2013). With regards to support structures, scouring around columns or abutments is of a great interest. It may lead to structural failures and thus much resources are directed toward monitoring and remediation (Prendergast and Gavin, 2014).

Because of such importance, there have been constant efforts to understand the transport process and its effect, in particular, with a focus on that in open channel flow. Hjelmfelt and Lenau (1970) presented an analytic solution for the concentration profile of sediment entrained from the bed in a uniform flow. The assumptions were that the distribution of the diffusion coefficient over the water depth is parabolic and that the depth-average velocity is constant. More recently, Kraus and Larson (2002) developed an analytic model to predict the bank encroachment rate over time, and it was applied to predict the infilling rate of channel in sand shore.

Laboratory experiments provide a means to validate and improve numerical solutions, which until recently, were limited to one- or two-dimensional flows. Delft Hydraulics Laboratory (1980) conducted a series of flume studies to extend its mathematical model for sediment transport over steep-sided trenches. Three different side slopes (1:3, 1:7, and 1:10) for the trench were tested. Its model showed good agreement with the measurements. However, the governing equations for hydrodynamics had been calibrated based on prior experiments. Van Rijn (1981) carried out a laboratory investigation to validate his mathematical model of sediment transport, as well as to compare with the analytical solution by Hjelmfelt and Lenau (1970). Wang and Ribberink (1986) validated a depth-integrated model for suspended sediment using a specially fabricated flume in which no re-suspension of sediment from the bed occurred.

With the advance of computing capabilities in the recent decades, simulation of sediment transport in complex flows was made possible through computational fluid dynamics (CFD) and it is increasingly being used. Wu et al. (2000) modeled three-dimensional flow in a 180°-channel bend, while also accounting for the secondary flows. The CFD tool used was FAST3D flow solver with the standard $k$-$\varepsilon$ turbulence model. The wall-function approach was taken to solve for the near-wall turbulence quantities. Khosronejad et al. (2007) simulated sediment transport around 90°- and 135°-channel bends. Finite volume method was used with a low-Reynolds number $k$-$\omega$ turbulence model and the standard $k$-$\varepsilon$ model.

This paper presents the results at the current stage of the authors' work to simulate the sediment transport process around bridge abutments in a channel bend. The work is being done by coupling three-dimensional hydrodynamics equations with sediment transport module. The numerical tool used is the in-house code FANS3D (Finite-Analytic Navier-Stokes code for 3D flow), based on the finite analytic method (Chen and Chen, 1984; Chen et al., 1990). For validation of the sediment transport module, the experimental data from van Rijn (1981) and Wang and Ribberink (1986) were used. The predictions showed good agreement with the measurements. The authors will further develop the model to incorporate scouring and bed morphology evolution modules.

[1] Ocean Engineering Program, Zachry Department of Civil Engineering, Texas A&M University, 3136 TAMU, College Station, Texas, 77843, USA

## HYDRODYNAMIC MODEL

### Governing Equations

The present numerical model solves three-dimensional unsteady, incompressible Reynolds-Averaged Navier-Stokes (RANS) equations. The equations can be written, in tensor notation (Wu et al, 2000),

$$\frac{\partial u_j}{\partial x_j} = 0 \tag{1}$$

$$\frac{\partial u_i}{\partial t} + \frac{\partial (u_i u_j)}{\partial x_j} = -\frac{1}{\rho}\frac{\partial p}{\partial x_i} + \frac{1}{\rho}\frac{\partial \tau_{ij}}{\partial x_j} + F_i \tag{2}$$

where $u_i$ = flow velocities; $\rho$ = fluid density; $p$ = pressure; $\tau_{ij}$ = deviatoric stresses; and $F_i$ = external force (e.g., gravity). The deviatoric stresses are defined as

$$\tau_{ij} = \rho(\nu + \nu_t)\left(\frac{\partial u_i}{\partial x_j} + \frac{\partial u_j}{\partial x_i}\right) - \frac{2}{3}\delta_{ij}k \tag{3}$$

where $\nu$ = kinematic viscosity; $\nu_t$ = eddy viscosity; $\delta_{ij}$ = Kronecker delta; and $k$ = turbulent kinetic energy.

In the present study, turbulence closure around smooth solid bodies is provided by the two-layer model of Chen and Patel (1988). Following this approach, the flow domain is divided into the near-wall region, which extends from the wall surface to a part of the outer region, and the fully turbulent outer region. This method allows for employing the one-equation eddy-viscosity model to resolve the turbulence quantities near the wall, while the standard $k$-$\varepsilon$ model is used for the rest of the flow domain.

The two-layer model greatly reduces the computing costs for simulations, as only the turbulent kinetic energy $k$ needs to be solved in the near-wall region. The relations used to determine the turbulence quantities are provided below.

- Near-wall Region (One-equation eddy-viscosity model):

$$\nu_t = c_\mu k^{1/2} \ell_\mu \tag{4}$$

$$\varepsilon = k^{3/2}/\ell_\varepsilon \tag{5}$$

$$\frac{\partial k}{\partial t} + \frac{\partial (u_j k)}{\partial x_j} = \frac{\partial}{\partial x_j}\left[\left(\nu + \frac{\nu_t}{\sigma_k}\right)\frac{\partial k}{\partial x_j}\right] + G - \varepsilon \tag{6}$$

- Turbulent Region (Standard $k$-$\varepsilon$ model):

$$\nu_t = c_\mu \frac{k^2}{\varepsilon} \tag{7}$$

$$\frac{\partial \varepsilon}{\partial t} + \frac{\partial (u_j \varepsilon)}{\partial x_j} = \frac{\partial}{\partial x_j}\left[\left(\nu + \frac{\nu_t}{\sigma_\varepsilon}\right)\frac{\partial \varepsilon}{\partial x_j}\right] + (c_{\epsilon 1} G - c_{\epsilon 2}\varepsilon)\frac{\varepsilon}{k} \tag{8}$$

where $\varepsilon$ = rate of energy dissipation; $\ell_\mu$ and $\ell_\varepsilon$ = mixing length scales; $G$ = production of $k$; and $\sigma_k$, $\sigma_\varepsilon$, $c_\mu$, $c_{\varepsilon 1}$, and $c_{\varepsilon 2}$ = model coefficients. Note that the standard transport equation for $k$ (6) is also employed in the turbulent region as well.

### Wall-Function Approach

When the roughness effects of the surface need to be taken into account, the wall-function approach from Wu et al. (2000) is used to resolve the near-wall flow. The first grid point away from the wall is placed in the logarithmic region ($30 < y^+ < 100$), and the velocity and the turbulence quantities are determined in terms of the shear velocity $u_\tau$ using the following relations:

$$\frac{U}{u_\tau} = \frac{1}{\kappa}\ln E y^+ \tag{9}$$

$$k = \frac{u_\tau^2}{c_\mu^{1/2}} \tag{10}$$

$$\varepsilon = \frac{u_\tau^3}{\kappa y} \tag{11}$$

where $U$ = total velocity parallel to the wall surface; κ = von Kármán constant; $y^+ = u_\tau y/\nu$ = viscous length; and $E$ = roughness parameter defined as

$$E = e^{[\kappa(B-\Delta B)]} \tag{12}$$

where $B = 5.2$ = constant; and $\Delta B$ = roughness parameter related to the equivalent roughness height $k_s$. Following Cebeci and Bradshaw (1977),

$$\Delta B = \begin{cases} 0, & k_s^+ < 2.25 \\ \left[B - 8.5 + \frac{1}{\kappa}\ln k_s^+\right]\sin[0.4258(\ln k_s^+ - 0.811)], & 2.25 \le k_s^+ < 90 \\ B - 8.5 + \frac{1}{\kappa}\ln k_s^+, & k_s^+ \ge 90 \end{cases} \tag{13}$$

$$k_s^+ = \frac{u_\tau k_s}{\nu} \tag{14}$$

The value of $k_s$ is chosen appropriately depending on the sediment particle size and the nature of the flow.

## SEDIMENT TRANSPORT MODEL

### Governing Equations

In this present study, the sediment concentration is treated as a passive scalar. The following transport equation, in tensor notation, is used to describe the concentration of the sediment suspended in flow (Wu et al., 2000):

$$\frac{\partial c}{\partial t} + \frac{\partial}{\partial x_j}\left[(u_j - \omega_s \delta_{j3})c\right] = \frac{\partial}{\partial x_j}\left[\left(\nu + \frac{\nu_t}{\sigma_c}\right)\frac{\partial c}{\partial x_j}\right] \tag{15}$$

where $c$ = volumetric suspended sediment concentration; $\omega_s$ = particle settling velocity; and $\sigma_c$ = Schmidt number. In this study, 1.0 was used as the value of $\sigma_c$. The tensor index of 3 indicates the vertical direction.

### Boundary Conditions

At the inlet, the actual measurements are used to prescribe the concentration profile. If measurements are not available, the equilibrium concentration profile following van Rijn (1986) or a uniform profile is used. At the outlet, zero-gradient condition is imposed. On the water surface, there can be no vertical sediment flux, thus:

$$\left(\nu + \frac{\nu_t}{\sigma_c}\right)\frac{\partial c}{\partial z} + \omega_s c = 0 \tag{16}$$

To describe the near-bed sediment concentration in cases where entrainment occurs, the approach by Wu et al. (2000) is followed, where the flow domain is divided into two zones: suspended load and bed load zones. The interface between the two zones is located at $z' = b$ (Here, the apostrophe indicates that the elevation was measured from the bed). The vertical flux of the sediment through the interface is then specified as the boundary condition using:

$$D_b - E_b = \omega_s(c_b - c_{b*}) \tag{17}$$

where $D_b$ = detrainment rate; $E_b$ = entrainment rate; $c_b$ = the sediment concentration; and $c_{b*}$ = the equilibrium concentration determined according to van Rijn (1986). The subscript $b$ indicates the quantities are determined at $z' = b$. The sediment concentration $c_b$ is calculated using Wu et al. (2000):

$$c_b = c_2 + c_{b*}\left[1 - e^{-(\omega_s \sigma_c / \nu_t)(z_2' - b)}\right] \tag{18}$$

where $c_2$ = the concentration at the first grid point away from the bed (Point 2); and $z_2'$ = elevation of the point 2 measured from the bed. In case there is no upward flux from the bed, zero-gradient condition is specified.

## NUMERICAL SCHEME

The present numerical method uses the finite analytic method as the discretization scheme in non-staggered, general curvilinear coordinate systems. The finite analytic method incorporates the local analytic solution to its numerical solutions. That is, an analytic solution of the governing differential equation is found for the interior point P, with the values at the surrounding points used for the local boundary conditions. In three-dimensional flow, the domain is divided into 27 grid points as depicted in Figure 1. For more detail the reader is referred to Chen and Chen (1984), Chen et al. (1990), and Chen et al. (2000).

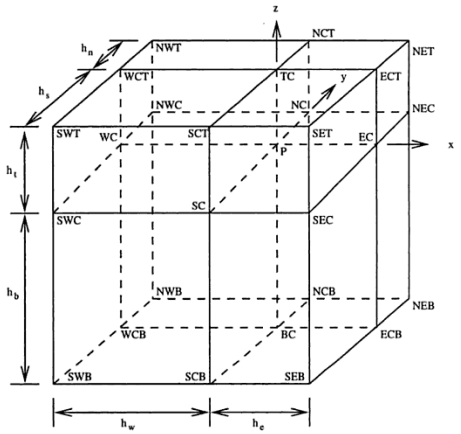


**Figure 1. The three-dimensional subdomain for the finite analytic method (Chen et al., 2000)**

The grid is generated with Chimera technique, which allows for embedding of non-matching grid blocks. As a result, flow solutions can be easily obtained for domains with very complex geometries. For velocity-pressure coupling, PISO/SIMPLER algorithms are used.

## VALIDATION

### Net Entrainment

The first validation case was the laboratory investigation by van Rijn (1981), which is characterized by net entrainment of sediment from the bed. In a flume, initially clear, fully-developed flow was introduced over the sediment bed and the sediment concentration was measured after the equilibrium condition was reached. The dimensions of the flume were 30 m × 0.5 m × 0.7 m (Length × width × height). The mean velocity of the inflow was 0.67 m/sec with the water depth being 0.25 m. The median diameter $d_{50}$ of the bed material (Sand) was 0.23 mm and its settling velocity was 0.022 m/sec. Syphon method was employed to sample the water-sediment mixture at five different depths at each of the four stations downstream of the inlet. The schematic of the experimental setup is provided in Figure 2.

The numerical simulation of the case used a computational domain with the dimensions 201 × 3 × 21 (i × j × k). The effects of the sidewalls were negligible and the flow was treated as two-dimensional. The mesh was refined near the lower boundary, thus improving the quality of the wall-function approach. The equivalent roughness height $k_s$ was set equal to 0.01 m. At the inlet, the velocity profile of the fully-developed flow was specified as the boundary condition, with zero sediment concentration. At the sidewalls zero-gradient boundary condition was used for all quantities.

The comparison between the simulation and the measurements is given in Figure 3. The figure shows the results at two different locations, $x/h = 4$ and $x/h = 40$ ($x$ and $h$ denote the longitudinal distance from the inlet and the water depth, respectively). The computed and measured sediment concentrations were normalized by a reference value of 3,000 mg/L. The vertical axis was also normalized, by the water depth. One can observe that the entrainment from the bed led to the increased concentration of suspended sediment between the two stations. For the normalized depth above around 0.5, very little or no amount of sediment concentration was predicted. Overall, the computed concentrations agree very well with the measurements.

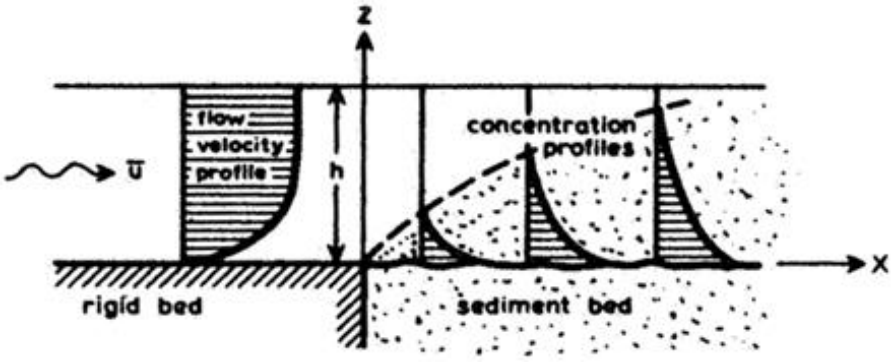


**Figure 2. Schematic of the experiment by van Rijn (1981).**

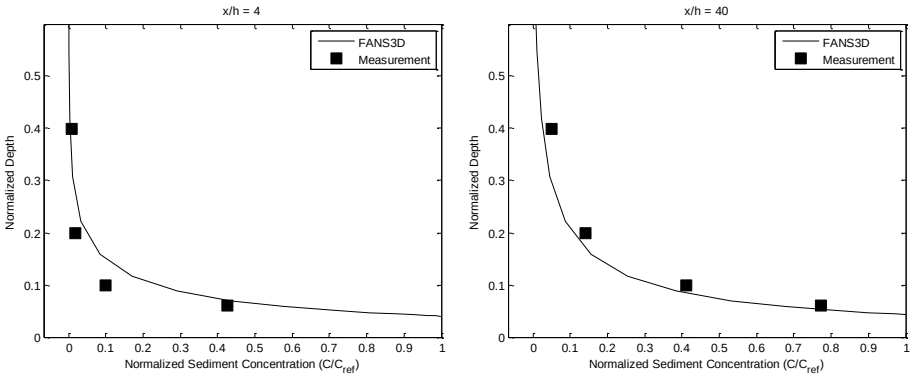


**Figure 3. Sediment concentration profiles with net entrainment from the bed.**

### Net Deposition

The measurements from another experimental study, conducted by Wang and Ribberink (1986) and involving zero entrainment from the bed, were used to verify the present model coupled with the sediment transport module.

The experiment was carried out in a straight flume with the dimensions 30 m × 0.5 m × 0.5 m (Length × width × height). The mean longitudinal velocity was 0.56 m/sec. A constant supply of sand was fed at the inlet of the flume, thus mimicking a steady, sediment-laden open channel flow. The characteristic diameter of the sediment $d_{50}$ was 0.095 mm and settling velocity $\omega_s$ was 0.0065 m/sec. Samples were taken using syphon at different distances downstream of the flume. To ensure that there was no re-entrainment of sediment from the bed, the channel bed was perforated and a compartment was placed below to capture and contain the sand particles, as shown in Figure 4.

With the physical specifications provided above, the experiment was simulated with a domain of the dimensions 201 × 3 × 51 (i × j × k). Just as the aforementioned test case, the flow was treated as two-dimensional. The measured distribution of suspended sediment at $x = 0.1$ m downstream from the inlet was taken as the inlet boundary values. At the bed, zero-gradient condition was used for the sediment concentration, since there was no upward flux.

The results are presented in Figure 5, for $x/h = 5$ and $x/h = 72$. It can be seen that the simulation predicted the actual concentrations very well in general. The concentration near the bed was over-predicted by the model. It is possible that an improved bed boundary condition is required to model the process with higher accuracy.

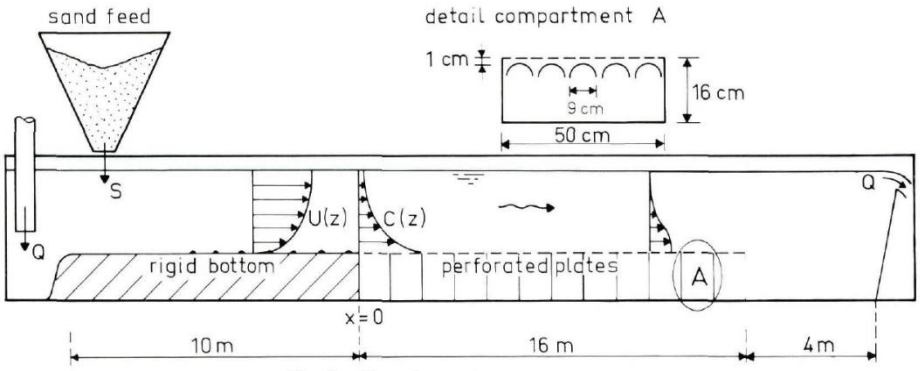


**Figure 4. Experimental setup by Wang and Ribberink (1986).**

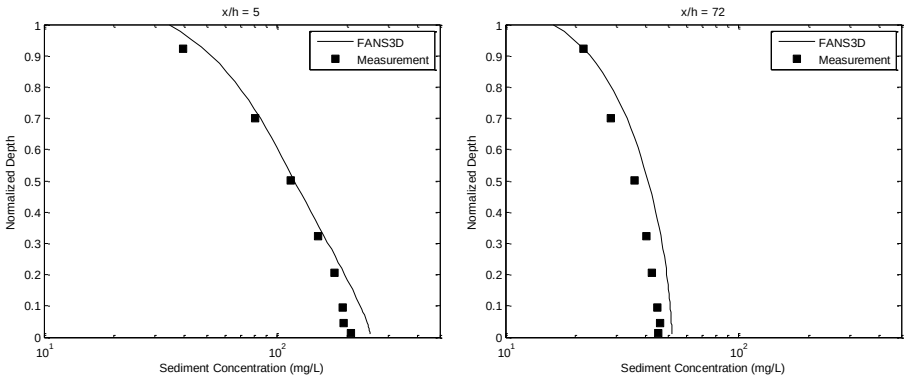


**Figure 5. Sediment concentration profiles without re-suspension from the bed.**

## APPLICATIONS

### Flow around Abutments

Before discussing the results of the present study, it is necessary to introduce the work by Briaud et al. (2009), which simulated the flow and scouring around abutments. Figure 6 shows the normalized velocity magnitude of the flow in a hypothetical channel bend. The inlet is located to the top left-hand corner of the figure.

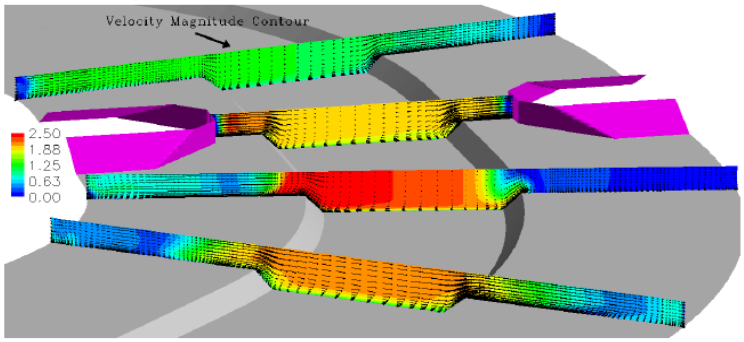


**Figure 6. Simulation of flow field reported by Briaud et al. (2009).**

Chen (2002) incorporated the equations for predicting the maximum bed shear stress into the present flow solver. Briaud et al. (2009) performed an extensive series of numerical simulations to analyze the influence of the various factors (e.g., the Reynolds number, channel contraction ratio, and abutment aspect ratio) and generated the time development of scour depth around the abutments. However, it should be noted that only clear-water scouring of cohesive soils was modeled, which neglects the presence of suspended sediment and its deposition. This very fact motivated the present authors to consider sediment-laden flow with non-cohesive sand as the bed material.

**Results**

With the sediment transport module validated by the experimental investigations, the study case described in the previous section was simulated, now with a specific amount of suspended sediment introduced at the inlet.

The geometry of this particular case was a 90°-channel bend with the radius of the bend equal to the width of the channel. The abutments, which were of the wing-wall type, were located in the middle of the bend. To simulate the flow, a computational domain consisting of eleven overlapping blocks, constructed with Chimera technique, was used. The total number of the grid points was 1,212,787. The grid dimensions were normalized by the water depth on the flood plane. The geometry of the domain is depicted in Figure 7.

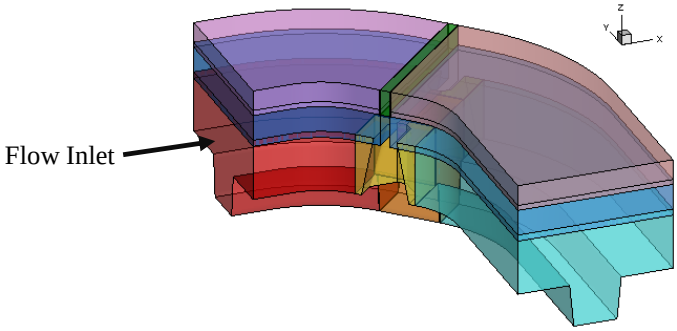


**Figure 7. Mesh of the present case, scaled by the factor of 10 in the vertical direction. Different coloring scheme is used for each block.**

At the inlet, uniform, normalized flow velocity of 1.0 was imposed as the boundary condition. No-slip condition was used at all solid surfaces. The distribution of suspended sediment was assumed to be uniform at the inlet and the value of 150 ppm was prescribed for the concentration. This setup mimics a homogeneous sediment plume entering the channel. However, during the simulation, no sediment was introduced to the domain until the flow reached a pseudo-fully developed state. The settling velocity $\omega_s$ of the sediment was set to equal 1% of the inlet velocity.

At all solid boundaries, including the bed, zero-gradient boundary condition was used for sediment concentration, which assumes no entrainment from the bed. This is a rather crude approach, considering the fact that in most open channel flows the bed is covered with sediments and re-suspension is common. However, at this particular stage of the study, the primary goal was to incorporate the transport equations of suspended sediment to the existing flow solver, and the bed boundary conditions will be improved in the future. Another important assumption was smooth solid surfaces. Accordingly, the two-layer model was used to resolve the near-wall turbulence. At the free surface zero sediment flux was enforced using Equation (16).

The simulated concentration of the suspended sediment and the magnitude of the total velocity in the domain of interest are shown in Figures 8 and 9, respectively. It should be noted that the figures do not reflect the depth-integrated values. Rather, they are plan views of a mid-section of the channel. The concentration is normalized by the inlet value. The three time steps – $t_1$, $t_2$, and $t_3$ – were chosen on the basis of capturing the transport of sediment through the channel.

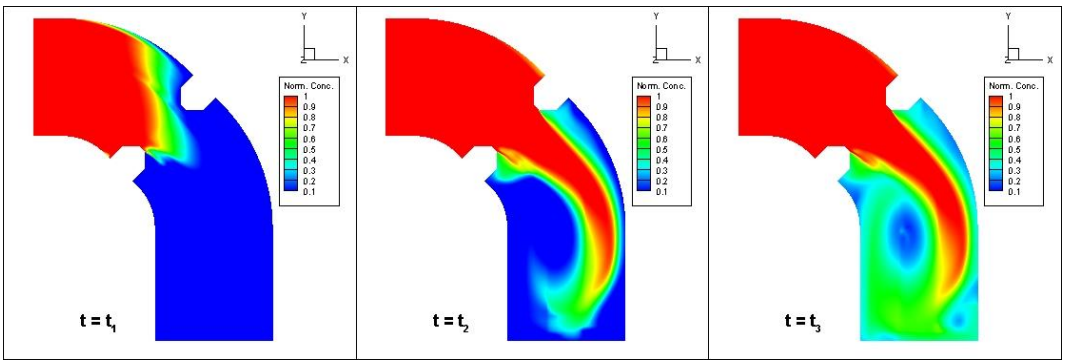


**Figure 8. Time series of normalized sediment concentration.**

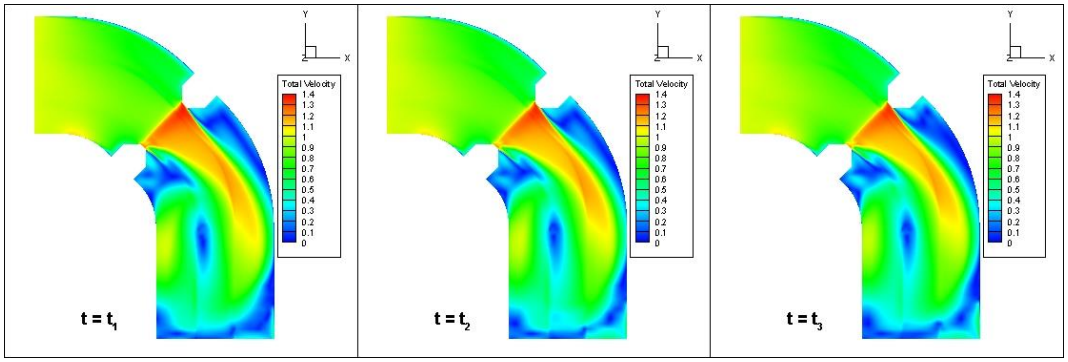


**Figure 9. Time series of total velocity.**

Figure 8 indicates that, with the given flow configurations, the sediment plume in the region upstream of the abutments had concentrations nearing the inlet condition. Figure 9 represents the pseudo-fully developed state of the flow. It was observed that the sediment transport occurred primarily by the convection of the flow, as can be seen by comparing the flow field and the sediment concentration downstream of the abutments (Figure 10).

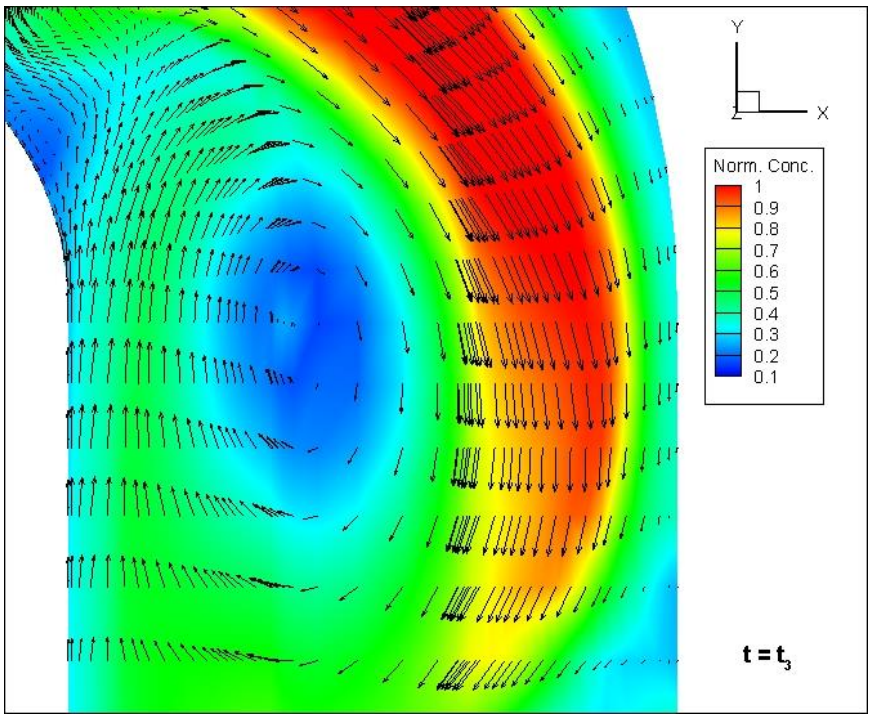


**Figure 10. Normalized sediment concentration overlaid with velocity vectors.**

Figure 10 shows the suspended sediment plume with the local velocity vectors downstream of the abutments at $t = t_3$. In this region, a swirl was formed due to the presence of the abutments and the curvature of the channel, and it dominated the sediment transport process.

## FUTURE WORKS

To further improve the current solution, the wall-function approach will be applied to account for the surface roughness effect of the bed. In turn, the flux of sediment between the bed load layer and the suspended load layer will be determined, which will lead to more accurate simulation of sediment transport. Ultimately, the authors plan to incorporate morphology evolution module to the current numerical model, which will provide the capability to simulate scouring around structures and bed elevation changes.

## CONCLUSION

Sediment transport has important implications in coastal engineering and related fields. As such, CFD is increasingly being used to investigate the process in complex flow domains. In the present study, FANS3D, a CFD solver for three-dimensional RANS equations, was coupled with a suspended sediment transport module. The concentration of suspended sediment is considered as a passive scalar. The two-layer model, which combines the one- and two-equation eddy-viscosity models, is used for turbulence closure on smooth solid surfaces, while the wall-function approach is employed to account for roughness effects in case of sediment-laden bed.

The new model was validated with two experimental studies. First, a flume study in which sediment was entrained from the bed in initially clear inflow was simulated. The mathematical formulation by Wu et al. (2000) was implemented to accurately model the flux of sediment particles at the bed. The computed sediment concentration values showed good agreement with the measurements. The second validation case involved no upward flux of sediment from the bottom boundary. The flume used in this study had perforated bed with a compartment to capture the sediment particles that settle through the holes. Overall, the numerical model predicted the sediment concentration profile with high accuracy. Both of the test cases were simulated as two-dimensional flow, since the sidewall effects were negligible and the advection was dominated by the flow in the longitudinal direction.

After validation, the model was then extended to the flow around abutments in channel bend. The domain configuration by Briaud et al. (2009) was used. Uniform sediment concentration profile was prescribed as the inlet boundary condition, and zero-gradient condition was used on all solid surfaces. The results indicated that the three-dimensional transport of suspended sediment was well simulated. The sediment plume in a swirl downstream of the abutments was notable. The present method is currently being extended to incorporate bed morphology evolution module.

## ACKNOWLEDGEMENT

The computational resources were provided by Texas A&M University's Supercomputing Facility (http://sc.tamu.edu).

## REFERENCES

Briaud, J.L., Chen, H.C., Chang, K.A., Oh, S.J., Chen, X. (2009). *Abutment scour in cohesive materials*. NCHRP Report 24-15(2), Transportation Research Board, National Research Council, Washington, D.C., USA.

Cebeci, T., and Bradshaw, P. (1977). *Momentum transfer in boundary layers*. Hemisphere, Washington, D.C., USA

Chen, C.J., Bernatz, R., Carlson K.D., and Lin, W. (2000). *Finite analytic method in flows and heat transfer*. CRC Press, New York, NY, USA.

Chen, C.J., and Chen, H.C. (1984). Finite analytic numerical method for unsteady two-dimensional Navier-Stokes equations. *Journal of Computational Physics*, 53.

Chen, H.C. (2002). Numerical simulation of scour around complex piers in cohesive soil. *First International Conference on Scour of Foundation*, College Station, Texas, USA.

Chen, H.C., and Patel, V.C. (1988). Near-wall turbulence models for complex flows including separation. *AIAA Journal*, 26(6).

Chen, H.C., Patel, V.C., and Ju, S. (1990). Solutions of Reynolds-Averaged Navier-Stokes equations for three-dimensional incompressible flows. *Journal of Computational Physics*, 88.

Delft Hydraulics Laboratory. (1980). *Computation of siltation in dredged trenches: Mathematical model*. Report R 1267 V, Delft, The Netherlands.

Hjelmfelt, A.T., and Lenau, C.W. (1970) Non-equilibrium transport of suspended sediment. *Journal of the Hydraulic Division*, HY 7.

Khosronejad, A., Rennie, C.D., Salehi Neyshabouri, S.A.A., and Townsend, R.D. (2007). 3D numerical modeling of flow and sediment transport in laboratory channel bends. *Journal of Hydraulic Engineering*, 133(10).

Kraus, N.C., and Larson, M. (2002). Analytical model of navigation channel infilling by cross-channel transport. *Proceeding of the 28th International Conference on Coastal Engineering*. ASCE, Virginia, USA.

Miller, M. "Costly dredging needs loom over Wellfleet Harbor." *Provincetown Banner* 6 Mar. 2013: Web <http://www.wickedlocal.com/wellfleet/news/x1433792079/Costly-dredging-needs-loom-over-Wellfleet-Harbor#axzz2QV5odiZa>

Prendergast, L.J., and Gavin, K. (2014). A review of bridge scour monitoring techniques. *Journal of Rock Mechanics and Geotechnical Engineering*, 6(2).

Rijn, L. C., van. (1981). *The development of concentration profiles in a steady, uniform flow without initial sediment load*. Report M1531, Part II, Delft Hydraulic Laboratory, Delft, The Netherlands.

Rijn, L. C., van. (1986). Mathematical modeling of suspended sediment in nonuniform flows. *Journal of Hydraulic Engineering*, 112(6).

Sánchez-Badorrey, E., Losada, M. A., and Rodero, J. (2008). Sediment transport patterns in front of reflective structures under wind wave-dominated conditions. *Coastal Engineering*, 55.

Wang, Z. B., and Ribberink, J. S. (1986). The validity of a depth-integrated model for suspended sediment transport, *Journal of Hydraulic Research*, 24(1).

Wu, W, Rodi, W., and Wenka, T. (2000). 3D numerical modeling of flow and sediment transport in open channels. *Journal of Hydraulic Engineering*, 126(1).